Aalborg Universitet

LiDAR-based 2D Localization and Mapping System using Elliptical Distance Correction Models for UAV Wind Turbine Blade Inspection

Nikolov, Ivan Adriyanov; Madsen, Claus B.

LiDAR-based 2D Localization and Mapping System using Elliptical Distance Correction Models for UAV Wind Turbine Blade Inspection

Ivan Nikolov[1], Claus Madsen[1]

[1]*Department of Architecture, Design, and Media Technology, Aalborg University, Rendsburggade 14, Aalborg, Denmark*
{iani, cbm}@create.aau.dk

Abstract: The wind energy sector faces a constant need for annual inspections of wind turbine blades for damage, erosion and cracks. These inspections are an important part of the wind turbine life cycle and can be very costly and hazardous to specialists. This has led to the use of automated drone inspections and the need for accurate, robust and inexpensive systems for localization of drones relative to the wing. Due to the lack of visual and geometrical features on the wind turbine blade, conventional SLAM algorithms have a limited use. We propose a cost-effective, easy to implement and extend system for on-site outdoor localization and mapping in low feature environment using the inexpensive RPLIDAR and an 9-DOF IMU. Our algorithm geometrically simplifies the wind turbine blade 2D cross-section to an elliptical model and uses it for distance and shape correction. We show that the proposed algorithm gives localization error between 1 and 20 cm depending on the position of the LiDAR compared to the blade and a maximum mapping error of 4 cm at distances between 1.5 and 3 meters from the blade. These results are satisfactory for positioning and capturing the overall shape of the blade.

1 INTRODUCTION

As robots and drones become widely used in different branches of the industry, a need for localization and mapping systems, which are able to work in non-ideal conditions, arises. The state of the art for drone simultaneous localization and mapping (SLAM) is most widely used both from monocular (Mur-Artal et al., 2015), stereo camera (Endres et al., 2012), LiDAR and laser scanners (Berger, 2013) (Zlot and Bosse, 2014) . A lot of SLAM algorithms for the outdoors are used together with GPS positioning and orientation from an inertial measurement unit (IMU) (Elseberg et al., 2012) (Shepard and Humphreys, 2014). SLAM algorithms work best in environments, which are rich in geometric features and vary significantly. The precision of these algorithms significantly suffers when the environment is too featureless or when there are insufficient number of points of interest, which requires the introduction of algorithm modifications, such as visual feature clustering (Negre et al., 2016) or combining camera and laser scanner depth data (Oh et al., 2015). When the number of points extracted from laser scanner is too low, due to sharp corners or thin surfaces, these modification cannot sustain a high enough performance. Similar problems are present when using drones in the wind energy sector for inspection of wind turbine blades. Wind turbine blades are normally located at over 100 meter heights and do not have any other landmarks around them. This, combined with the monochrome color of the blades and the lack of corners and other geometric features, makes autonomous localization of the drone and mapping the environment, hard.
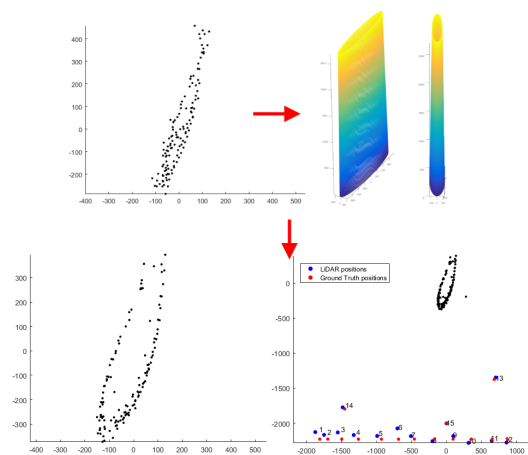

Figure 1: Our proposed localization and mapping solution using elliptical distance correction models.

We propose a cost-effective and easy to implement solution for localization and mapping the overall shape of the blade (Figure 1), designed to work in feature-poor wind turbine blade environments, with minimum prior information. Our system consists of the RPLIDAR scanner and the BNO055 9-DOF IMU for orientation. Our algorithm is based on the assumption that a blade is stopped in a vertical position, at either the top or bottom and is the only thing that is visible for the LiDAR. The algorithm uses prior information for the cross-section width and depth and it models the blade using primitive elliptical shapes, providing drone positioning relative to the blade in a much simpler way than conventional SLAM algorithms. The initial angle between the LiDAR and blade is found by using a 2D iterative closest point (ICP) algorithm and the angle heading is monitored and maintained using an IMU. Additionally we model the distance measurement and sampling errors of the RPLIDAR to boost the accuracy of the localization. We address the sunlight noise problem of the RPLIDAR with a hybrid hardware and software filtering solution. We perform initial ground-based tests on the system to determine its accuracy and error rate by comparing with ground truth manually measured positions. Additionally we estimate to what extent the algorithm can capture the overall shape of the 2D cross-section of the blade, using a ground truth cross-section. Both tests demonstrate that the system performs well even with a small number of points present from the scanned area and can be used for drone localization relative to the blade and generation of initial sparse 2D point clouds of the shape of the blade.

2 STATE OF THE ART

Drone inspection of wind turbine blades is a hot topic for the computer vision, automaton and robotics fields. The limited number of points of interest, the featureless and monochrome shape of the wind turbine blades and the required operational height, together with environment hazards like gusts of wind, blade swaying and weather changes make localization and mapping non-trivial problems. The research from (Morgenthal and Hallermann, 2014) shows that inspection by images can suffer significantly if the drone's localization and stabilization systems cannot compensate for environmental and weather changes. One way to tackle these problems is to have an initial fly-through, through which an occupancy map of the blade is created and which is then used for planning a flightpath, as suggested by (Schäfer et al., 2016). Another solution proposed by (Jung et al., 2015) can
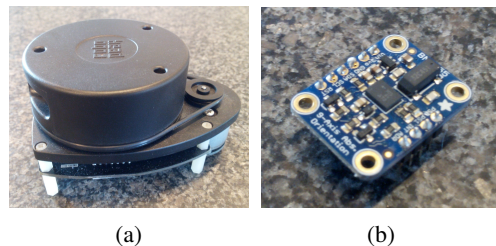

(a)   (b)

Figure 2: The hardware used for the proposed system - the RPLIDAR and the BNO055 9-DOF IMU

come not only from relying on a flying drone, but creating a hybrid flying and climbing vehicle, which uses a combination of sonar, IMU and LiDAR system to orient itself. Using a dynamic flightpath planning from a camera feed is a another strategy employed by (Galleguillos et al., 2015) and (Cordero et al., 2014), combining it together with navigation sensors like an IMU, GPS, barometer, etc.

We propose a localization and shape mapping system, which uses a LiDAR scanner and an IMU, plus a simplification of the wind turbine blade cross-section to a elliptical model for distance and shape correction. Our algorithm is based on the assumption that only the blade is visible at any time and works even when as little as 2 or 3 points are obtained from the scanned surface.

3 METHODOLOGY

3.1 Algorithm Overview

The proposed system, given in Figure 3, relies on prior shape information for a proper positioning. The prior information in our case, comes in the form of a model of the shape of the blade cross-section. Because finding a real world 3D model for each piece of the cross-section of the different kinds of blades in a problematic task, a simplified elliptical model is proposed. The elliptical model requires much less prior information and it gives centimeter precision results as shown in Section 4. Stray sunlight in the sensor causes detection noise, which is filtered away using a combination of hardware polarization and software k-nearest neighbors and line filters, before the LiDAR's raw data is used.

As an initial step, before the main localization algorithm is started, the angle between the blade and drone is calculated using readings from a low-cost LiDAR from (Slamtec, 2010), shown in Figure 2a and an 2D iterative closest point algorithm, as described in Subsection 3.4. The angle is used to rotate the elliptical model in the same direction as the blade and is
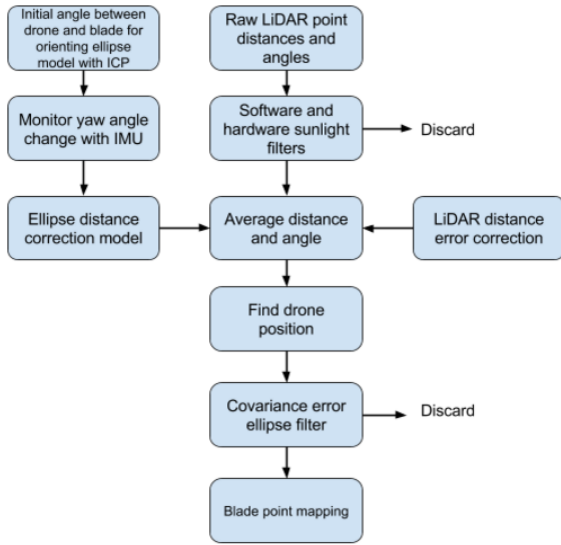
Figure 3: Algorithm and work pipeline overview. From raw LiDAR data and IMU orientation, to localization of the Li-DAR compared to the blade and mapping the points of the blade cross-section

then maintained with the readings from the IMU from (Adafruit, 2012), shown in Figure 2b. It is observed that the LiDAR exhibits errors in its readings, which change with the distance from the measured surface. To compensate for this error, we compare the measurements from the LiDAR and ground truth readings from a DISTO laser distance scanner. The differences are calculated, interpolated and smoothed out using a cubic spline and used as distance corrections.

Once the data is clear of noise, corrected from the distance errors and properly rotated, the elliptical distance correction model (EDC model) as seen in Subsection 3.3, together with the angle correction from the IMU, are applied. The localized drone position is filtered to remove false movement readings using a covariance ellipse error filtering, as proposed by (Friendly, 1991) and the blade points are mapped accordingly.

3.2 From Corrected LiDAR Data to Initial Drone Localization

The corrected output data from the RPLIDAR comes in polar coordinates. To position the data for each Li-DAR reading in a unified coordinate system, the data is first transformed to Cartesian coordinates. We assume that only the wind turbine blade is seen by the LiDAR at any given time, so the origin of the new Cartesian coordinate system is chosen to be the center of the scanned blade. We then wish to map everything to this coordinate system - both drone po-

sitions and blade surface points. Formula 1 is used for transforming the coordinates. Lets for a moment also assume that the centroid of the measured points from the LiDAR is a good approximation for the center of te blade, independent of where the LiDAR is compared to the blade. Naturally the are problems with that assumption and we will demonstrate how to compensate for that error in the next sections.

$$
\begin{aligned}
x_d &= 0 - D_{mean} \cdot sin(\alpha_{mean}) \\
y_d &= 0 - D_{mean} \cdot cos(\alpha_{mean})
\end{aligned}
\tag{1}
$$

Where the x_d and y_d are the drone coordinates in the new coordinate system, D_{mean} and α_{mean} are the mean distance and angle calculated from all detected points in a 360 degree reading. Once the LiDAR is self localized, compared to the blade, the LiDAR's position is used as a new center of a polar coordinate system to find the blade's previously detected points. The points are calculated in a Cartesian coordinate system using Formula 2.

$$
\begin{aligned}
x_i &= x_d + D_i \cdot sin(\alpha_i) \\
y_i &= y_d + D_i \cdot cos(\alpha_i)
\end{aligned}
\tag{2}
$$

Here x_i and y_i, are the coordinates of each of the data points in one reading and D_i and α_i are respectively their distances and angles. The center for calculating the blade points positions is the LiDAR's coordinates x_d and y_d, calculated in Formula 1. The whole process is visualized in Figure 4. The initial naive approach to localization and mapping yields some problems, such that the whole cross-section needs to be opened up. Additional processing is required to get the correct cross-section mapping and position localization. This is why we introduce the elllipse distance correction model (EDC model).

3.3 Elliptical Distance Correction Model (EDC model)

In real life the LiDAR does not measure the distance from the drone to the blade center, but to the exterior shell/body of the blade. The distance from the center of the blade to the exterior points that the LiDAR measures is not known to the LiDAR. This discrepancy leads to improper modeling of the surface shape of the blade and incorrect drone position calculation.

To be able to capture the proper shape of the blade profile and the proper LiDAR positions, an initial guess of the blade form is needed. The wing of a wind turbine has a very specific and hard to model shape, which changes with height. Each blade manufacturer has different specifications, numbering and
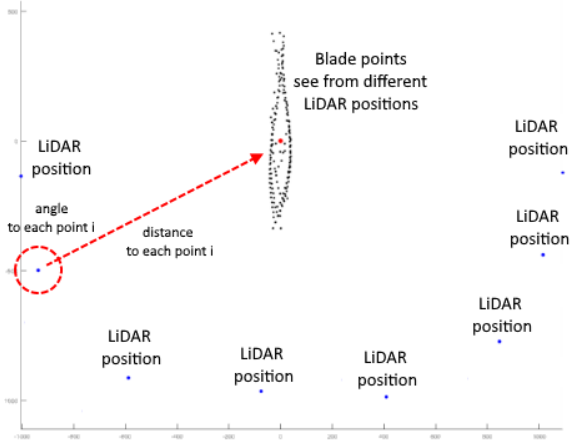
Figure 4: Initial drone localization. The corrected LiDAR data is transformed into a Cartesian coordinate system and the mean angle and distance are used to self-position the LiDAR compared to the blade. Once these positions are found they are used to find the blade points' positions. Eight LiDAR positions and the visible blade points are plotted in the Figure

shape mold and this information is not readily available. Therefore, an approximate simplified model is required as a substitute of the blade shape. The model can be further adjusted using known blade shapes. This requires making some assumptions:

- The LiDAR sees only the wind turbine blade;
- The wind turbine blade is stopped;
- The blade's cross-section width and depth are known;
- The vertical position of the drone is known.

An ellipse is suggested as such a simple geometrical shape, as it closely resembles the the blade cross-section, especially in the leading edge. To model properly the blade's size for the different heights, an ellipse shape is calculated for each height slice of the blade. The ellipse points are calculated using the Formula 3, where r_1 and r_2 are the two radii of the ellipse, which are selected based on the width and depth of the cross-section at the particular blade height and the angle $\beta \in [0 : 2\pi]$.

$$
\begin{aligned}
x_e &= 0 - r_1 \cdot sin(\beta) \\
y_e &= 0 - r_2 \cdot cos(\beta)
\end{aligned}
\tag{3}
$$

A full model of the blade is created and is saved in a table, for an easy access depending on the height of the drone, compared to the blade. Multiple elliptical models can be created for different blade dimensions and manufacturer models. A full 3D model can be seen in Figure 5.
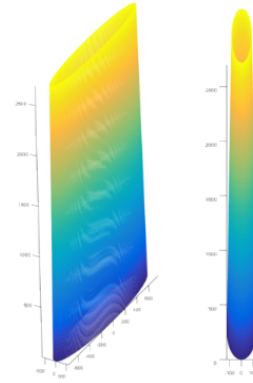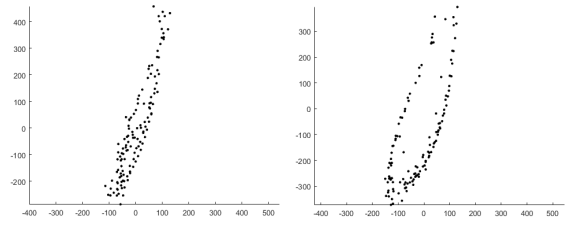

Figure 5: Elliptical model for correcting the LiDAR's position. The 3D model is created with interpolation of the two radii of the ellipse cross-section in Z direction, following the notion that wind turbine blades become smaller with height.

(a) Without EDC model   (b) With EDC model

Figure 6: Example mapping of the blade before and after the EDC model. The points' positions are corrected and the whole profile is opened up, especially the blade edge points.

For each point on the ellipse, the radius from the center to the point is calculated, as well as the angle on a circle with a center in (0,0). Each point on the ellipse is positioned in the same coordinate system as the points from the LiDAR. This way when the LiDAR position is calculated using the mean distance, the distance of the point on the ellipse with the closest angle to the mean angle of the LiDAR is added to it. This effectively pushes outwards the mean points and gives an initial guess on the shape of the blade. The difference can be seen when plotting the blade surface points before and after the elliptical correction, as seen in Figure 6. The correction is most noticeable on the points on the leading edge of the blade. The whole profile is opened up, representing the blade cross-section more closely.

Another problem becomes evident when using the EDC model - the ellipse needs to be initially oriented the same way as the blade profile. The rotation of the blade is initially unknown and needs to be determined before the correction can be applied to the localization and mapping.

3.4 Calculating Initial Angle Between Drone and Blade

The drone's yaw orientation is taken from the IMU unit. The angle between the detected blade profile from the LiDAR and the IMU connected to the drone is calculated. The initial angle is used to first orient the ellipse compared to the blade's orientation for the EDC model and also for keeping the mapped positions at the same heading. The change in the orientation of the wind turbine blade, while the LiDAR is scanning, is deemed too small, as it will be stopped from moving or rotating for the duration of the drone flight.

The angle between the blade and LiDAR can be calculated using ICP. Heuristically it is determined that at least 8 points are required in one reading for the ICP registration to be successful. The sides of the blade are better for registration than the edge, as they contain more points, which are spread more evenly. Because the success of the ICP depends on the quantity and quality of the registration points, a cubic spline is approximated to the scanned points. This way the scanned points are interpolated and any small noise position errors are smoothed over. A 2D ICP algorithm by (Bergström and Edlund, 2014) is used to register the LiDAR points to the prior elliptical model. A rigid registration is performed with only rotation and translation, as the ellipse is properly sized beforehand, using the initial information for the width and depth of the blade profile. The process can be seen in Figure 7.

Once the registration is completed, the rotation angle is used to rotate the EDC model. The angle is also added to the yaw angle measured by the IMU for use with the drone's yaw holding.
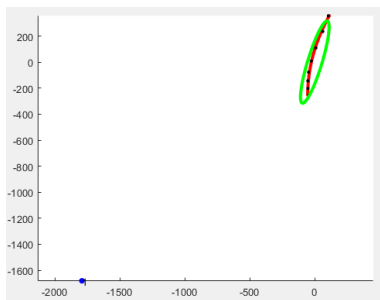

Figure 7: Initial ICP orientation of the EDC model. Blue points show the LiDAR's reading, red points are the approximated cubic spline and the green ellipse is the correction model

4 SYSTEM TESTS AND RESULTS

4.1 Localization Test

The first test aims to measure the localization accuracy of finding the position of the LiDAR compared to the blade. As the system is still in the prototyping stages, the measurements are done on the ground. A number of ground truth points are measured around the blade profile, ranging from 0.5m to 3.5m in distance from LiDAR to the blade leading edge. Two sets of fifteen positions are selected. The first set is with positions arranged in a circle and the second - in a line. These are selected, to demonstrate the system's performance with different scan patterns. Both sets contain outliers positions to verify the accuracy of the system in harder localization points, such as those far away or too close to the blade. The LiDAR is positioned on each of the ground truth points and the measured position is computed. Fifty readings are taken so any noisy measurements can be filtered away using the covariance ellipse error filtering. The Euclidean distance between each of the ground truth positions and measured LiDAR self positioning is computed, both with and without the elliptical distance correction model. The resultant error values from the first and second position datasets are given in Table 1 and the plotted LiDAR and blade points are given in Figure 8.

Table 1: Results from the first and second set of positions around the blade. The distance error(*mm*) between the ground truth position and the one measured by the LiDAR with the correction algorithm $E_{algorithm}$ and with only the raw data E_{raw}

	Dataset 1		Dataset 2	
Pos	E_{raw}	$E_{algorithm}$	E_{raw}	$E_{algorithm}$
1	88.36	76.01	213.10	119.22
2	259.96	210.01	183.81	79.88
3	187.54	119.01	221.20	111.19
4	221.32	118.63	199.42	88.59
5	228.45	104.67	221.51	75.40
6	386.52	81.49	372.17	153.79
7	263.29	64.54	333.90	64.49
8	152.99	16.18	306.11	41.51
9	84.32	12.20	276.03	43.08
10	47.17	18.26	150.44	66.08
11	138.62	42.21	136.81	18.49
12	341.87	51.91	110.82	45.54
13	183.16	135.09	75.77	34.39
14	180.57	110.27	131.25	36.79
15	285.28	84.67	248.22	4.59
Avg	**203.30**	**83.01**	**212.04**	**65.54**

(a) Dataset 1 without EDC model   (b) Dataset 1 with EDC model

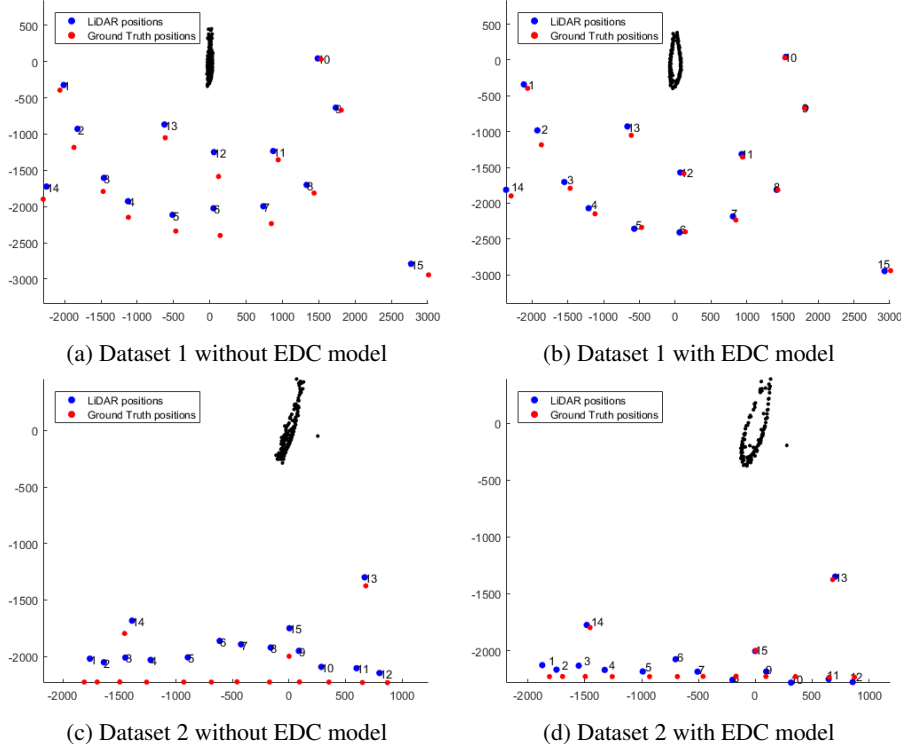(c) Dataset 2 without EDC model   (d) Dataset 2 with EDC model

Figure 8: Localization test using the first (8a and 8b) and second(8c and 8d) position datasets. The ground truth data is shown with red dots and the LiDAR calculated positions with blue dots. The mapped blade points are also plotted, for easier orientation

The results show that the system can provide a stable position estimate for where the drone is compared to the blade. The biggest differences between the measured and ground truth points come from positions where just a small amount of points from the surface can be seen in the Dataset 1 distances between ground truth and measurements in positions 3, 4, 5 and 13. In addition positions which are too far away from the blade surface exhibit both lower precision and accuracy, because insufficient points are sampled by the LiDAR, which makes faraway point angle and distance estimation jump around too much, as seen in the measurement in position 14 and 15 in Dataset 1. Some larger distances are observed in the first dataset, which can also be explained by problems with the yaw hold and small changes in the rotation of the LiDAR, as seen in position 2. In all positions, the introduction of the EDC model is shown to dramatically increase the accuracy of the localization, compared to just using the raw data. This is especially evident in the measurements 5 to 9 from Dataset 2.

4.2 Mapping Test

For testing the mapping capabilities of the LiDAR system, the blade profile is scanned with a Faro laser scanner and a high quality point cloud is created. A 2D cross-cut of the point cloud is then used as a ground truth, when comparing with the mapped blade point positions. In this test the LiDAR is placed in positions, forming a semicircle around the blade with three radii - 1.5 m, 2 m and 3 m, for testing the mapping capabilities from different distances. Additionally a post-processed mapping from 1.5 m, which has been registered to the elliptical prior model using the ICP algorithm is given, to demonstrate one way that the proposed algorithm can be extended to boost accuracy. The signed distances between each point of the two 2D point clouds is calculated. This is done using the free open source software CloudCompare (Girardeau-Montaut, 2003). From the distances, the mean and standard deviation of the distance distribution are calculated. The mean and standard deviation are given in Table 2 and the mapped blade surface points are given in Figure 9

The difference between the elliptical correction model and the blade cross-section becomes larger the farther away from the edge it goes, because the scanning is done only in a 180 degree semi-circle around the blade and details of the back of the blade are sparse. The front of the blade in the LiDAR scans shows a higher standard deviation and some noisy

Table 2: Mean value (μ) in *mm*, standard deviation (σ) in *mm²*, minimum (d_{min}) and maximum (d_{max}) in *mm* of the absolute distance metrics between the ground truth and the LiDAR mapped points from three distances to the blade (D_b) - 1.5, 2 and 3 meters

D_b	μ	σ	d_{min}	d_{max}
1.5	10.93	7.32	0.36	38.13
1.5 + ICP	9.32	6.92	0.24	31.038
2	14.89	9.19	0.62	38.40
3	15.65	9.23	1.31	39.30

(a) Ground truth (b) 1.5 meters (c) 1.5 meters + ICP (d) 2 meters (e) 3 meters
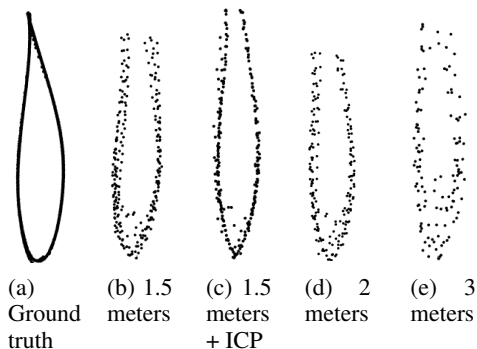
Figure 9: Mapped blade surface from the LiDAR, using the EDC model, together with the ground truth Faro scan and the post-processed 1.5 meter mapping using the ICP algorithm together with the elliptical prior model. The 2D point clouds get sparser and noisier the further away the LiDAR is.

points, because of the small amount of points seen from those angles. Even with these problems and the relatively small sampling density of the RPLIDAR, the proposed algorithm manages to restore the shape of the blade with centimeter accuracy. If a registration is done, the results get closer to the ground truth shape. This shows that the algorithm can be used as a proper substitute to SLAM.

5 CONCLUSION AND FUTURE WORK

We propose a low-cost, easy to implement drone localization and mapping system for wind turbine blades, using a cheap commercial LiDAR and an off-the-shelf IMU. Our system uses prior shape information in the form of elliptical distance correction model. It requires minimum prior information; it is computationally fast; simpler to implement than conventional SLAM; it can easily be extended and refined with additional training and provides satisfactory results. We demonstrate through ground based localization and a mapping tests that the system can self po-

sition and obtain mapping of the blade cross-cut with centimeter accuracy. In addition we propose a filter for removing noisy position information. Our algorithm also removes distance measurement errors and direct sunlight noise, so it can be used both outdoors and indoors.

As an extension of our work we propose an in-depth test of our system and algorithm against the state of the art SLAM algorithms performed on blade profiles, to verify the calculated accuracy of the system. Testing the algorithm using a "default" blade shape, which will better resemble the scanned blades, as a distance correction model is also suggested, as well as further adjusting it using training sets.

REFERENCES

Adafruit (2012). Adafruit bno055 9-dof imu. https://learn.adafruit.com/adafruit-bno055-absolute-orientation-sensor. Accessed: 2016-09-15.

Berger, C. (2013). Toward rich geometric map for slam: Online detection of planes in 2d lidar. *Journal of Automation Mobile Robotics and Intelligent Systems*, 7.

Bergström, P. and Edlund, O. (2014). Robust registration of point sets using iteratively reweighted least squares. *Computational Optimization and Applications*, 58(3):543–561.

Cordero, M., Trujillo, M., Ruiz, J., Jimenez, A., Diaz, L., and Viguria, A. (2014). Flexible framework for the development of versatile mav systems for multi-disciplinary applications. In *IMAV 2014: International Micro Air Vehicle Conference and Competition 2014, Delft, The Netherlands, August 12-15, 2014*. Delft University of Technology.

Elseberg, J., Borrmann, D., and Nüchter, A. (2012). 6dof semi-rigid slam for mobile scanning. In *2012 IEEE/RSJ International Conference on Intelligent Robots and Systems*, pages 1865–1870. IEEE.

Endres, F., Hess, J., Engelhard, N., Sturm, J., Cremers, D., and Burgard, W. (2012). An evaluation of the rgb-d slam system. In *Robotics and Automation (ICRA), 2012 IEEE International Conference on*, pages 1691–1696. IEEE.

Friendly, M. (1991). *SAS system for statistical graphics*. SAS Publishing.

Galleguillos, C., Zorrilla, A., Jimenez, A., Diaz, L., Montiano, Á., Barroso, M., Viguria, A., and Lasagni, F. (2015). Thermographic non-destructive inspection of wind turbine blades using unmanned aerial systems. *Plastics, Rubber and Composites*.

Girardeau-Montaut, D. (2003). Cloudcompare. http://www.cloudcompare.org/. Accessed: 2016-09-15.

Jung, S., Shin, J.-U., Myeong, W., and Myung, H. (2015). Mechanism and system design of mav (micro aerial vehicle)-type wall-climbing robot for inspection of wind blades and non-flat surfaces. In *Control, Automation and Systems (ICCAS), 2015 15th International Conference on*, pages 1757–1761. IEEE.

Morgenthal, G. and Hallermann, N. (2014). Quality assessment of unmanned aerial vehicle (uav) based visual inspection of structures. *Advances in Structural Engineering*, 17(3):289–302.

Mur-Artal, R., Montiel, J., and Tardós, J. D. (2015). Orb-slam: a versatile and accurate monocular slam system. *IEEE Transactions on Robotics*, 31(5):1147–1163.

Negre, P. L., Bonin-Font, F., and Oliver, G. (2016). Cluster-based loop closing detection for underwater slam in feature-poor regions. In *2016 IEEE International Conference on Robotics and Automation (ICRA)*, pages 2589–2595. IEEE.

Oh, T., Kim, H., Jung, K., and Myung, H. (2015). Graph-based slam approach for environments with laser scan ambiguity. In *Ubiquitous Robots and Ambient Intelligence (URAI), 2015 12th International Conference on*, pages 139–141. IEEE.

Schäfer, B. E., Picchi, D., Engelhardt, T., and Abel, D. (2016). Multicopter unmanned aerial vehicle for automated inspection of wind turbines. In *2016 24th Mediterranean Conference on Control and Automation (MED)*, pages 244–249. IEEE.

Shepard, D. P. and Humphreys, T. E. (2014). High-precision globally-referenced position and attitude via a fusion of visual slam, carrier-phase-based gps, and inertial measurements. In *2014 IEEE/ION Position, Location and Navigation Symposium-PLANS 2014*, pages 1309–1328. IEEE.

Slamtec (2010). Slamtec rplidar. http://www.slamtec.com/en. Accessed: 2016-09-15.

Zlot, R. and Bosse, M. (2014). Efficient large-scale 3d mobile mapping and surface reconstruction of an underground mine. In *Field and service robotics*, pages 479–493. Springer.